

OPEN

CD206⁺ tumor-associated macrophages promote proliferation and invasion in oral squamous cell carcinoma via EGF production

A. S. M. Rafiul Haque¹, Masafumi Moriyama^{1,2}, Keigo Kubota³, Noriko Ishiguro¹, Mizuki Sakamoto¹, Akira Chinju¹, Keita Mochizuki¹, Taiki Sakamoto¹, Naoki Kaneko¹, Ryusuke Munemura¹, Takashi Maehara¹, Akihiko Tanaka¹, Jun-Nosuke Hayashida¹, Shintaro Kawano¹, Tamotsu Kiyoshima⁴ & Seiji Nakamura¹

Tumor-associated macrophages (TAMs) promote tumor progression and inhibit anti-tumor immune response by producing various mediators and preferentially express CD163, CD204, and CD206. However, the role of these TAM subsets in oral squamous cell carcinoma (OSCC) remains unclear. Here we investigated the expression and function of TAM subsets in OSCC, especially in cancer cell proliferation. Biopsy sample from 44 patients with OSCC were examined for the expression of TAM markers and EGF by immunohistochemistry. EGF production of TAM subsets isolated from OSCC patients was assessed by flow cytometry. We also examined the effect of conditioned medium from TAM subsets on the proliferation of OSCC cells. CD163⁺ cells were detected diffusely all over the tumor and connective tissue area, while CD204⁺ and CD206⁺ cells were mainly detected in/around the tumors. Flow cytometric analysis found that CD206⁺ TAMs strongly produced EGF compared with CD163⁺ and CD204⁺ TAMs. Cell proliferation and invasion of OSCC cells cultured with conditioned medium of CD206⁺ TAMs were strongly enhanced and inhibited by anti-EGFR. The number of CD206⁺ TAMs positively correlated with worse clinical prognosis. Our results revealed differences in localization and EGF production among these TAM subsets. CD206⁺ TAMs might play a critical role in the proliferation of OSCC via EGF production.

Oral squamous cell carcinoma (OSCC) is a tumor of the oral cavity epithelial in origin that affects more than 400,000 people per year worldwide. The mortality rate has not been improved over decades, and the 5 year survival rate is under 70%¹. Tumor microenvironments comprise cancer cells and various normal cells including immune, inflammatory, and stromal cells^{2–4}. Several studies indicated that M2 macrophages infiltrate into the tumor microenvironment and promote tumor immunosuppression, cancer progression, angiogenesis, invasion and metastasis. This phenotype of macrophage called tumor-associated macrophage^{5–7}.

CD163⁻, CD204⁻, and CD206⁻ positive macrophages are significantly associated with poor prognosis, pTNM staging and lymph node metastasis in lung cancer^{8–10}, and thus CD163, CD204, and CD206 are considered as useful markers for activation of TAMs. CD163 is a hemoglobin scavenger receptor that is specifically expressed in the monocyte-macrophage system. Recently, it has been found that soluble CD163 also may be a potential diagnostic parameter for monitoring the activity of macrophage in inflammatory diseases¹¹. CD204 is a Class A scavenger receptor that is involved in the pathogenesis of atherosclerosis and the pattern recognition of pathogen

¹Section of Oral and Maxillofacial Oncology, Division of Maxillofacial Diagnostic and Surgical Sciences, Faculty of Dental Science, Kyushu University, Fukuoka, Japan. ²OBT Research Center, Faculty of Dental Science, Kyushu University, Fukuoka, Japan. ³Department of Oral-Maxillofacial Surgery, Dentistry and Orthodontics, The University of Tokyo Hospital, Tokyo, Japan. ⁴Laboratory of Oral Pathology, Division of Maxillofacial Diagnostic and Surgical Sciences, Faculty of Dental Science, Kyushu University, Fukuoka, Japan. A. S. M. Rafiul Haque and Masafumi Moriyama contributed equally. Correspondence and requests for materials should be addressed to M.M. (email: moriyama@dent.kyushu-u.ac.jp)

infection¹². CD206 is a macrophage mannose receptor 1 that is strongly expressed in prostate adenocarcinoma, and the number of CD206-positive TAM was correlated with poor prognosis of the disease¹³.

TAMs secrete extensive amounts of proangiogenic growth factors including epidermal growth factor (EGF) are considered as the most potent source of EGF in tumor microenvironment^{14,15}. EGF acts as a chemotactic factor in the tumor microenvironment and promotes the motility and invasion of tumor cells, consequently accelerating metastasis^{16,17}. EGF was also shown to promote cancer cell proliferation in cultured breast cancer cells¹⁸.

In this study, we investigated the expressions of CD163⁺, CD204⁺, and CD206⁺ TAMs in OSCC and their association with clinical outcomes. We also examined the levels of EGF production by each TAM subset and the effects of the proliferation of OSCC cells.

Materials and Methods

Ethics statement. The Institutional Review Board of Center for Clinical and Translational Research of Kyushu University Hospital (IRB serial number: 27–362) authorized the study design and methods. The study was performed along with the permitted guidelines. Written informed consent was obtained from all patients and/or their legal guardians on admission and accordingly before their involvement in this study.

Patients. Forty-four enrolled patients with primary OSCC who were treated in the Department of Oral and Maxillofacial Surgery at Kyushu University Hospital from 2005 to 2018 (mean age, 66.5 ± 10.3 years; range 35–89 years; 25 male and 19 female patients). After taking the biopsy sample, 4% buffered formalin solution was used to fix the specimens and then implanted in paraffin to make blocks. 5- μm thick sections were prepared from the paraffin-embedded specimens, hematoxylin and eosin (H&E) were used to stain the sections to confirm the diagnosis and histologic grade by a professional oral pathologist. Stage of the tumor was classified as stated in the TNM classification of the International Union Against Cancer. WHO classification was used to determine the tumor histologic grade. According to the Yamamoto-Kohama clinical classification of OSCC the pattern of tumor invasion was assessed from the H&E-stained specimens as: grade 1 = well-defined borderline; grade 2 = cords, less-marked borderline; grade 3 = groups of cells, no distinct borderline; and grade 4 = diffuse invasion (4C = cord-like type invasion; 4D = widespread type invasion). Patients type and the clinicopathological characteristics of tumor are shown in Table 1.

Immunohistochemical analysis. First, we deparaffinized the sections in xylene and then hydrated by graded series of ethanol, the detail of the staining procedure were mentioned in our previous study¹⁹. Following primary antibodies were used to incubate the sections for overnight at 4 °C. Primary antibodies included rabbit anti-CD3 (Clone SP7; ab16669, Abcam, Tokyo, Japan, 1:200 dilution), rabbit anti-CD20 (Clone EP459Y; ab78237, Abcam, Tokyo, Japan, 1:100 dilution), mouse anti-CD163 (Clone 10D6; Novocastra, Newcastle, UK, 1:400 dilution), mouse anti-CD204 (Clone SRA-C6; TransGenic Inc, Kumamoto, Japan, 1:200 dilution), mouse anti-CD206 (Clone 5C11; Abnova, Taipei, Taiwan, 1:300 dilution), and rabbit anti-EGF (Clone ab9695; Abcam, Tokyo, Japan, 1:30 dilution). Antibody was washed by TBST and as a chromogen 100–400 μl DAB (Peroxidase Stain DAB Kit, nacalai tesque, Kyoto, Japan) was applied to each section. Finally, Mayer's hemalum solution (Merck KGaA, Darmstadt, Germany, 1:4 dilution) was used for counterstain and then sections were washed two times for 5 min each in dH₂O. After dehydration, sections were mounted with coverslips. The numbers of CD3-, CD20-, CD163-, CD204-, CD206-, and EGF-positive cells were counted in 4 mm² sections from five independent high-power microscopic fields (400 \times , 0.0625 μm^2).

Double and triple immunofluorescence analysis. The slides were microwaved in AR6 buffer (Opal-4 Color Manual IHC kit; PerkinElmer, Waltham, MA, USA) and cooled for 30 min. Sections were then incubated in Antibody Diluent/Blocking Buffer (Opal-4 Color Manual IHC kit; PerkinElmer) for 10 min at room temperature and then incubated with primary antibodies (as listed before). Double staining was performed with CD3/EGF, CD20/EGF, CD163/EGF, CD204/EGF, and CD206/EGF, and triple staining was performed with CD163/CD204/CD206 for 2.5 h at room temperature. Samples were washed three times in TBST for 2 min each and then incubated in Polymer HRP (Ms + Rb), (Opal-4 Color Manual IHC kit; PerkinElmer) Samples were rinsed three times in TBST for 2 min each and then incubated in Opal Fluorophore working solution (Opal-4 Color Manual IHC kit; PerkinElmer) for 10 min at room temperature. Samples were rinsed in TBST, microwaved in AR6 buffer and then mounted with VECTASHIELD MOUNTING MEDIUM FOR FLUORESCENCE WITH DAPI (Vector Laboratories, Burlingame, CA, USA). In double staining, CD3, CD20, CD163, CD204, and CD206 were labeled with Opal 520 Fluorophore (Green) and EGF was labeled with Opal 570 Fluorophore (Red). In triple staining CD163, CD204, and CD206 were labeled with Opal 520 Fluorophore (Green), Opal 570 Fluorophore (Red), Opal 690 Fluorophore (White), respectively. For taking photomicrographs we used a light microscope with a digital camera (BZ-9000 series; Keyence, Tokyo, Japan). The ratio of EGF-positive cells in immune cells was defined as the ratio of the number of each EGF⁺ immune cells (yellow) to the whole number of each immune cells (yellow and green) in a 4-mm² field of view, from five separate areas.

Flow cytometric analysis. For detection of intracellular EGF, 5 OSCC patients peripheral blood mononuclear cells (PBMCs) (5×10^5 cells/ml) were collected and cultured in PBS and then stimulated with 40 ng/ml PMA (phorbol 12-myristate 13-acetate; Wako, Tokyo, Japan), 4 $\mu\text{g/ml}$ ionomycin (Ionomycin Calcium; Wako) and Brefeldin A Solution (BioLegend, San Diego, CA, USA, 1:1000 dilution) for 6 h in a moistened chamber at 37 °C with 5% CO₂ supply.

Next, the harvested cells were washed with eBioscience Flow Cytometry Staining Buffer (Thermo Fisher Scientific, Waltham, MA, USA). After rinsing, the cells were incubated at normal temperature for 20 min in dark with PE anti-human CD163 antibodies (Clone GHI/61, IgG1, κ ; BioLegend), FITC anti-human CD204 antibodies (Clone REA460, IgG1; Miltenyi Biotec, Bergisch, Gladbach, Germany), and PerCP/Cy5.5 anti-human

	Case (%)	CD163+ cells (/HPF)	P-value	CD204+ cells (/HPF)	P-value	CD206+ cells (/HPF)	P-value
Age[†]							
≤65	26 (59.1)	34.0 ± 20.4	N.S.	41.4 ± 20.5	N.S.	44.8 ± 9.9	N.S.
65 <	18 (40.9)	32.8 ± 20.4		42.0 ± 21.0		44.4 ± 10.1	
Gender[†]							
Male	25 (56.8)	27.8 ± 16.6	N.S.	41.4 ± 24.6	N.S.	47.0 ± 11.5	N.S.
Female	19 (43.2)	37.0 ± 20.4		33.4 ± 20.4		48.0 ± 7.3	
Primary site[†]							
Tongue	24 (54.5)	25.4 ± 15.3	N.S.	33.0 ± 13.4	N.S.	47.0 ± 10.9	N.S.
Gingiva	10 (22.7)	36.8 ± 26.2		43.2 ± 31.5		47.5 ± 9.7	
Buccal mucosa	6 (13.6)	40.3 ± 11.2		58.4 ± 27.3		48.5 ± 5.8	
Oral floor	3 (6.8)	39.0 ± 9.2		38.0 ± 4.9		47.0 ± 12.6	
Lymph node	1 (2.3)	35.0		24.0		44.0	
Clinical stage[*]							
I	7 (15.9)	23.4 ± 18.0	N.S.	33.0 ± 13.8	N.S.	47.0 ± 10.7	0.024 r = 0.339
II	20 (45.5)	32.0 ± 17.1		37.5 ± 19.2		47.0 ± 9.4	
III	8 (18.1)	28.3 ± 12.7		51.1 ± 29.7		48.0 ± 11.3	
IV	9 (20.4)	38.0 ± 22.2		39.0 ± 28.0		50.0 ± 7.3	
T classification[*]							
T1	8 (18.1)	22.6 ± 18.9	N.S.	33.0 ± 17.4	N.S.	46.0 ± 10.0	0.047 r = 0.301
T2	23 (52.3)	33.0 ± 15.4		37.0 ± 16.7		47.0 ± 9.0	
T3	7 (15.9)	24.6 ± 13.2		46.2 ± 28.0		47.0 ± 11.7	
T4	6 (13.6)	43.1 ± 26.1		68.2 ± 26.6		50.1 ± 8.4	
Cervical nodal metastasis[†]							
+	7 (15.9)	37.0 ± 22.9	N.S.	38.0 ± 29.1	N.S.	50.0 ± 7.0	0.029
-	37 (84.1)	31.0 ± 17.0		39.0 ± 22.5		47.0 ± 9.8	
Local recurrence[†]							
+	11 (25.0)	36.0 ± 16.3	N.S.	41.4 ± 29.9	N.S.	47.0 ± 12.1	N.S.
-	33 (75.0)	32.0 ± 18.9		38.0 ± 20.7		48.0 ± 8.9	
Distant metastasis[†]							
+	4 (9.0)	45.3 ± 40.3	N.S.	69.8 ± 40.0	N.S.	52.5 ± 4.2	N.S.
-	40 (90.9)	32.5 ± 14.7		38.0 ± 20.0		47.0 ± 10.0	
Histological grade[†]							
Grade 1	28 (63.6)	24.4 ± 15.6	N.S.	35.7 ± 25.2	N.S.	47.0 ± 10.2	N.S.
Grade 2	15 (34.1)	42.0 ± 17.5		41.4 ± 20.7		48.0 ± 9.7	
Grade 3	1 (2.3)	69.0		39.0		50.0	
Mode of invasion (YK criteria)[*]							
Grade 1	6 (13.6)	20.5 ± 15.2	N.S.	31.0 ± 14.6	N.S.	47.5 ± 12.9	N.S.
Grade 2	10 (22.7)	34.5 ± 16.5		30.8 ± 8.1		47.5 ± 9.3	
Grade 3	13 (29.5)	42.6 ± 22.5		48.0 ± 26.9		49.0 ± 10.0	
Grade 4C	9 (20.4)	27.8 ± 9.0		43.0 ± 27.0		41.0 ± 8.4	
Grade 4D	6 (13.6)	35.8 ± 14.7		45.7 ± 25.7		34.5 ± 11.4	

Table 1. Association of tumor-associated macrophages (TAMs) with clinicopathologic characteristics in OSCC. *Spearman's rank correlation coefficient, [†]Mann-Whitney *U*-test and Wilcoxon signed-rank test. N.S., not significant.

CD206 antibodies (Clone 15-2, IgG1, κ; BioLegend). We used PE mouse IgG1, κ (BioLegend), FITC REA Control (S)-VioBright antibodies recombinant human IgG1 (Miltenyi Biotec), and PerCP/Cy5.5 mouse IgG1, κ (BioLegend) as isotype control antibodies. Cells were fixed and permeabilized in Fixation Buffer (BioLegend) and Intercellular Staining Perm Wash Buffer (10X) (BioLegend), followed by staining with APC anti-hHB EGF (Clone # 125923, IgG_{2A}; R&D System, Minneapolis, MN, USA). APC mouse IgG_{2A} (R&D System) served as a negative control. We used BD FACVerse™ Flow Cytometer (Franklin Lakes, New Jersey, United States) and BD FACSuite™ software for acquiring and analyzing FACS data.

Separation and culture of TAM subsets. PBMCs from a healthy donor were collected and by using EasySep™ Human Monocyte Isolation Kit (STEMCELL Technologies Inc, Vancouver, Canada) CD14⁺ monocytes were isolated. Then, the isolated CD14⁺ cells (5 × 10⁶ cells/ml) were differentiated into M2 macrophages by CellXVivo Human M2 Macrophage Differentiation Kit (R&D System) in a humidified chamber at 37 °C in a 5% CO₂ atmosphere for 6 days. After differentiation M2 macrophages were collected and washed.

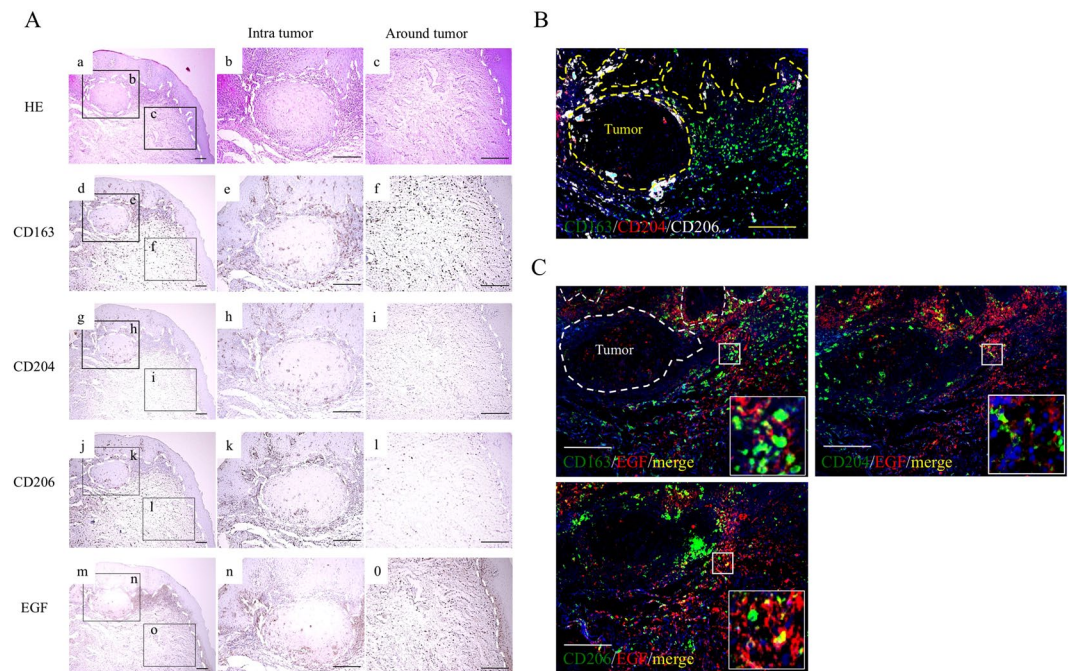


Figure 1. Distribution of tumor-associated macrophages (TAMs) and epithelial growth factor (EGF) in oral squamous cell carcinoma (OSCC) patients. **(A)** Representative images of paraffin sections in/around tumors stained with H&E (a–c) and CD163 (d–f), CD204 (g–i), CD206 (j–l), and EGF (m–o) antibodies (brown). Counterstaining with Mayer’s hematoxylin is shown in blue. Scale bars, 100 μm . **(B)** Triple immunofluorescence staining was performed with CD163 (green), CD204 (red), and CD206 (white); nuclei were stained with DAPI (blue). Scale bars, 50 μm . **(C)** Double immunofluorescence staining performed with EGF (red) and CD163, CD204 or CD206 (green); nuclei were stained with DAPI (blue). Merged TAM markers and EGF images (yellow). The higher magnifications are displayed at the lower right. Scale bars, 50 μm .

Once counting, the cells were transfer in three 15 ml tubes. Right after, the cells were incubated with FITC anti-human CD163 antibodies (BioLegend), FITC anti-human CD204 antibodies (Miltenyi Biotec), and FITC anti-human CD206 antibodies (BioLegend) at 4 °C for 10 min in dark. MACS buffer (Miltenyi Biotec) was used to rinse the sample and then incubated with Anti-FITC MicroBeads (Miltenyi Biotec) for 15 min at 4 °C. Subsequently samples were washed and sorted in three different following TAM subsets; CD163⁺, CD204⁺, and CD206⁺ cells by manual magnetic-activated cell sorting procedure with MiniMACSTM Separator and Starting Kit, (Miltenyi Biotec) as stated in manufacturer’s instruction manual and earlier reports²⁰. After that each TAM subsets (2.5 × 10⁶ cells/ml) were cultured in Dulbecco’s Modified Eagle Medium: Nutrient Mixture F-12 (DMEM/F12) (Life Technologies Corporation, Carlsbad, CA, USA) with 2% FBS (Sigma-Aldrich, St. Louis, MO, USA) and 1% Penicillin-Streptomycin Mixed Solution (nacalai tesque, Kyoto, Japan). Every 3 days of culture, we collected the conditioned medium (CM) from the TAM subsets and stored the CM at 4 °C.

Enzyme-linked immunosorbent assay (ELISA). We used CM of CD163⁺, CD204⁺, and CD206⁺ cells as samples and DMEM (Life Technologies Corporation) with 2% FBS (Sigma-Aldrich) as the control for ELISA. We concentrated the CM using the Amicon[®] Ultra-15 3K (Merck Millipore, Burlington, MA, USA); a total of 15 ml of culture medium was centrifuged at 4000 × g in 25 °C for 20 min to make 200 μl of sample. The samples were examined using the Human EGF Quantikine ELISA Kit (R&D Systems, Minneapolis, MN, USA) in accordance with the manufacturer’s guidelines, and EGF concentration was measured by using the Multiskan FC microplate reader (Thermo Fisher Scientific, Waltham, MA, USA) at a wavelength of 450 nm.

Cell division assay. The OSCC cell lines HSC-2, SQUU-A, and SQUU-B were used in this study. Establishment of the HSC-2 cell line was done from metastatic cervical lymph node lesions of OSCC of floor of the mouth²¹, while SQUU-A and SQUU-B cell lines were established from recurrent tongue cancer of the same patient by orthotopic implantation²². Cells were stained with CFSE Cell Division Assay Kit (Cayman Chemical Company, Ann Arbor, MI, USA) as reported in the manufacturer’s instructions and then cultured in DMEM (Life Technologies Corporation) with 10% FBS (Sigma-Aldrich) for various days. After that Cell division was analyzed by using BD FACSVerseTM Flow Cytometer.

Cell proliferation assay. HSC-2 cells (1 × 10⁴/well) were cultured in a 96-well dish with CM from CD163⁺, CD204⁺, and CD206⁺ cells for 4 days at 37 °C with 5% CO₂ with or without Anti-EGFR antibody (Clone ab231; Abcam, Tokyo, Japan 1:100 dilution). DMEM (Life Technologies Corporation) with 2% FBS (Sigma-Aldrich) was used as a control. Cell proliferation was examined by the XTT Cell Proliferation Assay Kit (Cayman Chemical

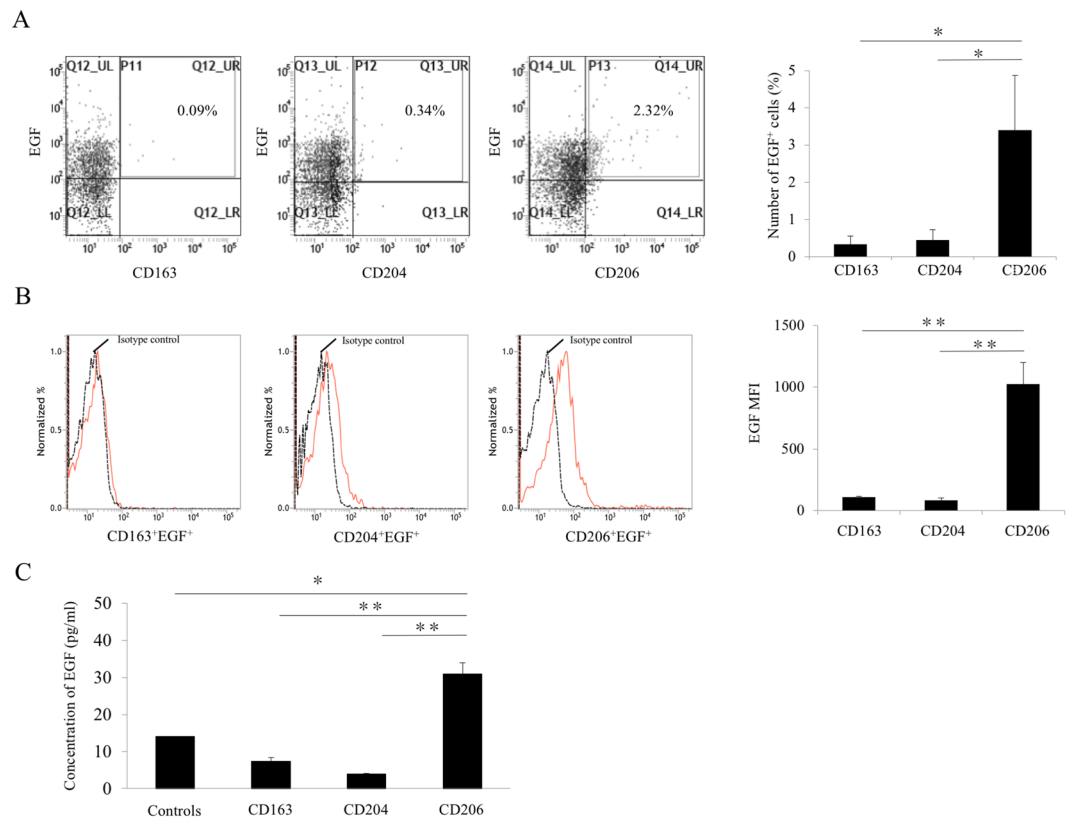


Figure 2. EGF expression on TAM subsets in OSSC patients. **(A)** The number of EGF⁺ cells and **(B)** EGF expression (MFI, mean fluorescent intensity) on TAM subsets. The number and MFI of EGF⁺ cells were determined using flow cytometry ($n = 5$ for each subset). **(C)** The concentration of EGF in conditioned medium (CM) of each TAM subset was determined by enzyme-linked immunosorbent assay ($n = 7$ for each subset). Cells were cultivated as described in Materials and Methods. Controls were only DMEM 2% FBS without TAM subset. Statistically significant differences between groups were determined by Kruskal-Wallis test (* $P < 0.05$, ** $P < 0.01$).

Company, Ann Arbor, MI, USA) as mentioned by the manufacturer. The color absorbance of each sample was read by using a Multiskan FC microplate reader (Thermo Fisher Scientific, Waltham, MA, USA) at a wavelength of 450 nm.

Cell invasion assay. HSC-2 cell lines were cultured for 4 days in CM of CD163⁺, CD204⁺, and CD206⁺ cells and used for invasion assays by using Corning® BioCoat™ Matrigel® Invasion Chambers (Corning Incorporated, Corning, NY, USA) As follows the product's guidelines, three Matrigel and three control inserts were prepared for a 24 well culture dish. The CM (750 μ l) of CD163⁺, CD204⁺, and CD206⁺ TAM was used as a chemoattractant in each well subsequently and the insert was filled with 500 μ l of DMEM (Life Technologies Corporation) without serum and HSC-2 cell line (2.5×10^4 cells/insert). The cells were cultured for 22 hours in a humid chamber with 5% CO₂ atmospheric state at 37 °C temp. Then the inserts were removed from the wells and Matrigel was cleaned off. After that cells were fixed with 100% methanol (Junsei Chemical Co.,Ltd., Tokyo, Japan) and then stained by Mayer's hemalum solution (Merck KGaA, Darmstadt, Germany, 1:4 dilution) and Tissue-Tek eosin (Sakura Finetek Japan Co., Ltd, Tokyo, Japan) (Supplementary Method 1).

The numbers of cells on the membrane were counted in 4 mm² sections from five different high-power microscopic fields (400 \times ; 0.0625 μ m²). The average number of cells in the Matrigel insert membrane was divided with the average number of cells in the control insert membrane, and then multiplied with 100 to calculate the invasion percentage.

Statistical analysis. JMP software version 11 (SAS Institute, NC, USA) was used to carry out the statistical analyses. The significant differences between each group were assessed by Mann-Whitney U test, Kruskal-Wallis test, Wilcoxon test, and Spearman's rank correlation coefficient test. For progression-free survival (PFS) and disease-specific survival (DSS) evaluation Kaplan-Meier method was used and by using the Cox hazard test curve comparisons were calculated. Receiver operating characteristic (ROC) curve was used to evaluate the sensitivity, specificity and the areas under the curve (AUC). In all analyses, P values ≤ 0.05 were considered statistically significant.

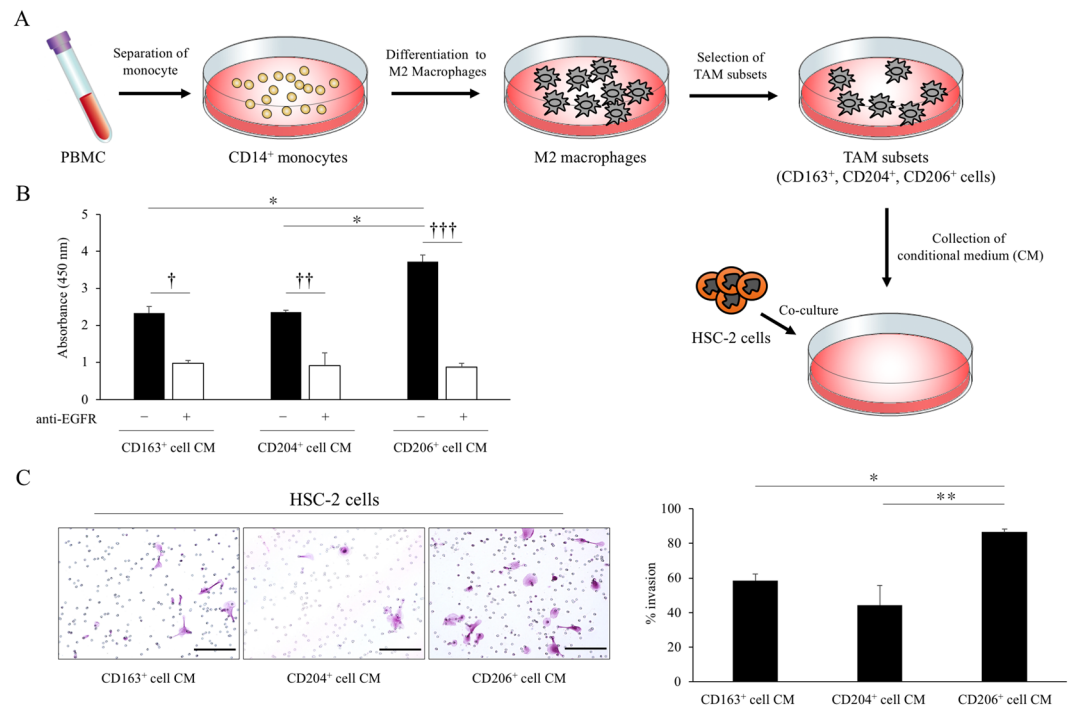


Figure 3. Effect of proliferation and invasion in OSCC cell lines by co-culture with CM of TAM subsets. **(A)** Scheme and representative image for the co-culture of HSC-2 cells and CM of TAM subsets for 4 days ($n = 3$ for each subset). Cells were cultivated as described in Materials and Methods. **(B)** Viability of HSC-2 cells co-cultured with CM of TAM subsets with/without anti-EGFR antibody ($n = 3$ for each subset). **(C)** Invasion activity of HSC-2 cells co-cultured with CM of TAM subsets ($n = 3$ for each subset). Scale bars, 100 μm . Statistically significant differences between groups were determined by Kruskal-Wallis test ($*P < 0.05$) and Mann-Whitney U -test ($^{\dagger}P < 0.05$, $^{**}P < 0.01$, $^{***}P < 0.001$).

Results

Expression of TAM markers in OSCC tissues. Immunohistochemical staining was performed to evaluate the localization of TAM markers (CD163, CD204, and CD206) in OSCC tissues. Representative histology results are shown in Fig. 1. Expression of CD163 was diffusely detected in tumor stroma and around tumors, while expressions of CD204 and CD206 were mainly detected in and around tumors (Fig. 1A). Triple immunofluorescence staining confirmed that the distribution of these TAM markers in OSCC tissues was quite different (Fig. 1B).

Co-localization of TAM markers and the EGF proangiogenic growth factor in OSCC tissues. Immunohistochemical staining showed that the expression of EGF, a proangiogenic growth factor, was strongly detected throughout the tumors and epithelial cells (Fig. 1A). To clarify whether TAM subsets express EGF, double immunofluorescence staining with TAM markers and EGF was performed. As shown in Fig. 1C, all three TAM markers were partially co-localized with EGF. Moreover, lymphocytes (CD3 or CD20-positive cells) also were partially co-localized with EGF, but EGF was mainly expressed on TAMs, especially CD206⁺ TAMs (Supple Fig. 1).

Expression levels of proangiogenic growth factor produced by TAMs. To determine whether CD163, CD204, and CD206-positive cells expressed EGF, we isolated the three TAM subsets in PBMCs from 7 patients with OSCC and examined the expression levels of EGF. As shown in Fig. 2A,B, CD206⁺ cells expressed higher levels and numbers of EGF intracellularly compared with CD163⁺ and CD204⁺ cells. These results suggest a difference in the expression of EGF among the TAM subsets. To determine the production of EGF by each TAM subset, we also evaluated the concentration of EGF in the CM of each TAM subset. The concentration of EGF in CM of CD206⁺ cells was higher than that of CD163⁺ and CD204⁺ cells (Fig. 2C).

Association of TAMs with proliferation and invasion of OSCC cell lines. We next examined the effect of co-culturing CM of the TAM subsets (CD163⁺, CD204⁺, and CD206⁺ cells) with OSCC cells *in vitro* (Fig. 3A). We first evaluated cell division rates of three OSCC cell lines, including SQUU-A, SQUU-B, and HSC-2, and found that HSC-2 cells showed a high cell division rate compared with SQUU-A and SQUU-B cells (Supple Fig. 2). We therefore selected HSC-2 cells for subsequent co-culture experiments.

Cell proliferation assays revealed a highly increased viability of HSC-2 cells co-cultured with CM of CD206⁺ cells in comparison with cells co-cultured with CD163⁺ and CD204⁺ cell CM. Furthermore, we found that anti-EGFR antibody significantly reduced the viability of HSC-2 cells co-cultured with CM of TAM subsets,

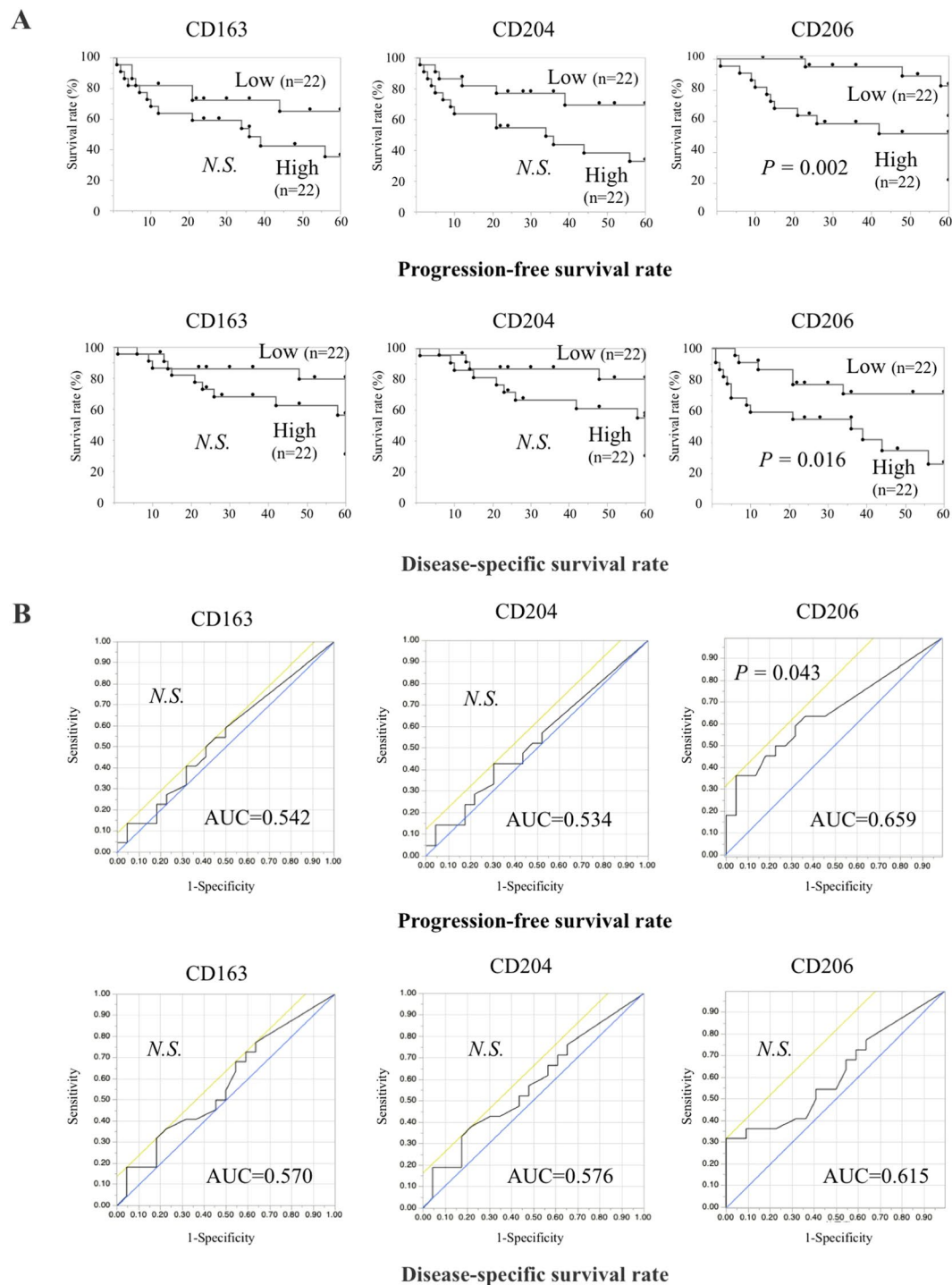


Figure 4. Survival curves according to the expression of TAM subsets in OSCC. Survival rates were calculated by the Kaplan-Meier method with high versus low expression of CD163⁺, CD204⁺, or CD206⁺ TAMs. The classifications are described in the Materials and Methods section. Statistically significant differences between groups were determined by log-rank test (A) and ROC curve (B).

especially CD206⁺ cells (Fig. 3B). We also confirmed the effect of EGFR expression on HSC2 cells co-cultured with each TAM subset CM, and there were no significant differences among TAM subsets (Supple Fig. 3). Similar results were observed in invasion assays. The invasion activity of HSC-2 cells co-cultured with CM of CD206⁺ cells was more enhanced than the invasion of cells co-cultured with CD163⁺ and CD204⁺ cell CM (Fig. 3C).

Association of TAM subsets with clinical and pathological findings of OSCC patients. We next examined the association of TAM subsets with the clinicopathologic factors of OSCC patients. Each number of TAM subsets was counted by single staining. As shown in Table 1, the number of CD163⁺ and CD204⁺ cells did

		Progression-free survival rate		Disease-specific survival rate	
		HR (95% CI)	P value	HR (95% CI)	P value
Age (y)	<65 vs 65≤	1.52 (0.62–4.06)	0.36	1.72 (0.70–4.61)	0.24
Sex	Male vs female	1.02 (0.42–2.53)	0.96	1.05 (0.42–2.54)	0.91
Pathologic tumor status	pT1 + T2 vs T3 + T4	1.45 (0.54–3.57)	0.43	2.06 (0.77–5.09)	0.15
Pathologic node status	N- vs N+	0.38 (0.06–1.35)	0.15	0.36 (0.06–1.25)	0.12
Pathologic metastasis status	M0 vs M1	2.46 (0.70–6.74)	0.14	2.48 (0.71–6.77)	0.14
Stage	1 + 2 vs 3 + 4	1.05 (0.41–2.55)	0.91	1.34 (0.52–3.24)	0.53
WHO grade	1 vs 2 + 3	1.17 (0.46–2.84)	0.72	1.40 (0.55–3.39)	0.47
YK status	1 + 2 vs 3 + 4	3.03 (1.11–10.6)	0.03*	3.31 (1.21–11.6)	0.02*
EGF positive cells	Low vs high	1.67 (0.68–4.46)	0.26	1.78 (0.72–4.73)	0.21
CD163 positive cells	Low vs high	2.21 (0.85–5.58)	0.10	2.03 (0.83–5.42)	0.12
CD204 positive cells	Low vs high	2.32 (0.95–6.18)	0.06	2.14 (0.87–5.71)	0.09
CD206 positive cells	Low vs high	3.28 (1.1–14.1)	0.03*	3.29 (1.1–14.1)	0.03*

Table 2. Univariate analysis of progression-free survival and disease-specific survival in advanced stage. Statistically significant differences between groups were determined by Cox proportional hazard model (* $P < 0.05$). HR, hazard ratio; CI, confidence interval.

not show significant associations with any clinicopathologic finding. However, the OSCC patients with clinical stage, clinical T classification, and cervical nodal metastasis showed a significant increase only in the number of CD206⁺ cells.

Associations of TAM subsets with clinical outcomes and prognosis of OSCC patients. To evaluate the correlation between TAM subsets and the clinical prognosis of OSCC patients, survival rates were estimated by using Kaplan-Meier method. We divided the OSCC patients into low and high expression groups according to the mean number of TAM subsets. In the PFS and DDS, there were no significant differences in low and high CD163⁺ and CD204⁺ expression. However, patients with high CD206⁺ expression had a significantly more unfavorable outcome than those with low expression group (Fig. 4A). According to the above results, we speculate that CD206 is a potential indicator to describe the malignancy of OSCC, so we performed statistical analysis by the ROC curve of clinical prognosis. The AUC area of DFS-related ROC curves of CD163⁺, CD204⁺, and CD206⁺ expression were 0.542, 0.534, and 0.659, respectively, and that of DSS-related ROC curves of CD163⁺, CD204⁺, and CD206⁺ expression were 0.570, 0.576, and 0.615, respectively (Fig. 4B). These results indicate higher sensitivity and specificity of CD206⁺ expression for adverse prognosis. Moreover, univariate analysis revealed that PFS and DSS were associated with YK criteria and number of CD206⁺ cells (Table 2).

Together these results suggest that CD206⁺ cells play a key role in the invasion and metastasis in OSCC.

Discussion

In 1908, Metchnikov *et al.* first demonstrated that macrophages were efficient phagocytes and played major roles in inflammation and natural cellular immunity²³. In the 1970's, macrophages were considered to be notable effector cells that functioned in the cytotoxic killing of tumor cells²⁴. Macrophages are divided into two functionally distinct subtypes: classically activated (M1) macrophages, which are stimulated by T helper type 1 (Th1) responses, and alternatively activated (M2) macrophages, which stimulated by Th2 responses^{7,8}. M1 macrophages produce pro-inflammatory cytokines and contribute to tumor suppression, whereas M2 macrophages express anti-inflammatory cytokines and have been shown to contribute to tumors by promoting angiogenesis, immunosuppression and activation of tumor cells²⁵. Recent studies have described M2-polarized macrophages as TAMs, which highly express markers, including CD163, CD204, and CD206^{26–28}.

CD163 is a member of the scavenger receptor cysteine-rich family class B and is mainly expressed on mature tissue macrophages²⁹. The main function of CD163 is the binding of the hemoglobin-haptoglobin complex. In addition, CD163-positive macrophages infiltrate in inflammatory tissues and were involved in the resolution of inflammation³⁰.

CD204 is a prototypic member of a family of structurally different transmembrane receptors conjointly termed as scavenger receptors and is primarily expressed on macrophages and dendritic cells³¹. CD204 recognizes modified lipid proteins, and exogenous pathogen-associated molecular patterns, and apoptotic cells. We previously reported that CD163⁺CD204⁺TAMs promote T-cell apoptosis and immunosuppression via IL-10 and programmed death-ligand 1 in OSCC patients¹⁹.

CD206 contributes to lipid metabolism, atherogenesis, and metabolic processes³². CD206 is a C-type lectin, alternatively termed as the macrophage mannose receptor, that is, generally expressed by tissue macrophages, dendritic cells, and specific lymphatic or endothelial cells. CD206 plays an important role in immune homeostasis, but its high expression has been increasingly detected in the tumor microenvironment³³.

TAMs play important functions in the tumor microenvironment, with roles in invasion, proliferation, and metastasis³⁴. Several studies indicated that TAMs secrete various kinds of cytokines including growth factor, for example EGF and IL-6, and EGF strongly induces tumor cell proliferation^{15–17}.

In this present study, we examined the expression of TAM subsets in OSCC tissues and the relationship between the expression of TAM markers and EGF production and tumor progression. Immunohistochemical staining demonstrated marked differences in the localizations of CD163⁺, CD204⁺, and CD206⁺ cells in OSCC tissues. Interestingly, CD206⁺ cells, from PBMCs of OSCC patients, strongly produced EGF compared with the other TAM subsets. In addition, OSCC cells showed high viability and invasion activity after co-culture with CM of CD206⁺ cells and a significant decrease in their viability with anti-EGFR antibody. These results suggest that CD206⁺ TAMs might play an important role in the proliferation and invasion of OSCC via EGF secretion. Goswami *et al.*³⁵ found a paracrine loop between breast carcinoma cells and macrophages through EGF and colony stimulating factor 1 production, leading to increased carcinoma cell invasion. While this paracrine loop might be also involved in the invasion activity in OSCC cells, further examinations are needed to clarify the expression of other cytokines secreted by TAM subsets in OSCC.

Next, we examined the involvement of TAMs in the prognosis of OSCC patients. The numbers of CD206⁺ TAMs in OSCCs were positively correlated with several clinicopathologic factors including clinical stage, clinical T classification, mode of invasion, and cervical nodal metastasis. Notably, a high number of CD206⁺ TAMs was significantly correlated with poor prognosis. Recently, Dong *et al.*³⁶ reported that the high presence of CD206⁺ TAMs in hepatocellular carcinoma markedly correlated with aggressive tumor phenotypes and were associated with poor prognosis. These results were consistent with our results. In contrast, in adult T-cell leukemia/lymphoma, both CD204⁺ and CD206⁺ TAMs were not associated with clinical outcome³⁷. These controversial results may be due to different tumor types.

In conclusion, we demonstrated that CD206⁺ TAMs promote proliferation and invasion of OSCC cells via EGF and high numbers of CD206⁺ TAMs predict unfavorable clinical prognosis in OSCC patients. However, it is still necessary to elucidate the involvement of other cytokines secreted by TAMs in the tumorigenesis. A more detailed knowledge of the role of each TAM subset could lead to the development of novel pharmacological approaches targeting TAMs or their products, and inhibiting the tumor progression and metastasis.

References

- Petersen, P. E. Oral cancer prevention and control—the approach of the World Health Organization. *Oral Oncol* **45**, 454–460, <https://doi.org/10.1016/j.oraloncology.2008.05.023> (2009).
- Hanahan, D. & Weinberg, R. A. The hallmarks of cancer. *Cell* **100**, 57–70 (2000).
- Hanahan, D. & Weinberg, R. A. Hallmarks of cancer: the next generation. *Cell* **144**, 646–674, <https://doi.org/10.1016/j.cell.2011.02.013> (2011).
- Sonnenschein, C. & Soto, A. M. The aging of the 2000 and 2011 Hallmarks of Cancer reviews: a critique. *J Biosci* **38**, 651–663 (2013).
- Jacques, A., Bleau, C., Turbide, C., Beauchemin, N. & Lamontagne, L. Macrophage interleukin-6 and tumour necrosis factor- α are induced by coronavirus fixation to Toll-like receptor 2/heparan sulphate receptors but not carcinoembryonic cell adhesion antigen 1a. *Immunology* **128**, e181–192, <https://doi.org/10.1111/j.1365-2567.2008.02946.x> (2009).
- Varney, M. L., Johansson, S. L. & Singh, R. K. Tumour-associated macrophage infiltration, neovascularization and aggressiveness in malignant melanoma: role of monocyte chemotactic protein-1 and vascular endothelial growth factor-A. *Melanoma Res* **15**, 417–425 (2005).
- Gordon, S. Alternative activation of macrophages. *Nat Rev Immunol* **3**, 23–35, <https://doi.org/10.1038/nri978> (2003).
- Chung, F. T. *et al.* Tumor-associated macrophages correlate with response to epidermal growth factor receptor-tyrosine kinase inhibitors in advanced non-small cell lung cancer. *Int J Cancer* **131**, E227–235, <https://doi.org/10.1002/ijc.27403> (2012).
- Ohtaki, Y. *et al.* Stromal macrophage expressing CD204 is associated with tumor aggressiveness in lung adenocarcinoma. *J Thorac Oncol* **5**, 1507–1515, <https://doi.org/10.1097/JTO.0b013e3181eba692> (2010).
- Zhang, B. *et al.* M2-polarized tumor-associated macrophages are associated with poor prognoses resulting from accelerated lymphangiogenesis in lung adenocarcinoma. *Clinics (Sao Paulo)* **66**, 1879–1886 (2011).
- Shigeoka, M. *et al.* Cyr61 promotes CD204 expression and the migration of macrophages via MEK/ERK pathway in esophageal squamous cell carcinoma. *Cancer Med* **4**, 437–446, <https://doi.org/10.1002/cam4.401> (2015).
- Komohara, Y. *et al.* Clinical significance of CD163(+) tumor-associated macrophages in patients with adult T-cell leukemia/lymphoma. *Cancer Sci* **104**, 945–951, <https://doi.org/10.1111/cas.12167> (2013).
- Hu, W. *et al.* Alternatively activated macrophages are associated with metastasis and poor prognosis in prostate adenocarcinoma. *Oncol Lett* **10**, 1390–1396, <https://doi.org/10.3892/ol.2015.3400> (2015).
- Murdoch, C., Muthana, M., Coffelt, S. B. & Lewis, C. E. The role of myeloid cells in the promotion of tumour angiogenesis. *Nat Rev Cancer* **8**, 618–631, <https://doi.org/10.1038/nrc2444> (2008).
- O'Sullivan, C., Lewis, C. E., Harris, A. L. & McGee, J. O. Secretion of epidermal growth factor by macrophages associated with breast carcinoma. *Lancet* **342**, 148–149 (1993).
- Segall, J. E. *et al.* EGF stimulates lamellipod extension in metastatic mammary adenocarcinoma cells by an actin-dependent mechanism. *Clin Exp Metastasis* **14**, 61–72 (1996).
- Wilson, S. E. *et al.* Effect of epidermal growth factor, hepatocyte growth factor, and keratinocyte growth factor, on proliferation, motility and differentiation of human corneal epithelial cells. *Exp Eye Res* **59**, 665–678, <https://doi.org/10.1006/exer.1994.1152> (1994).
- Wyckoff, J. B., Segall, J. E. & Condeelis, J. S. The collection of the motile population of cells from a living tumor. *Cancer Res* **60**, 5401–5404 (2000).
- Kubota, K. *et al.* CD163(+)CD204(+) tumor-associated macrophages contribute to T cell regulation via interleukin-10 and PD-L1 production in oral squamous cell carcinoma. *Sci Rep* **7**, 1755, <https://doi.org/10.1038/s41598-017-01661-z> (2017).
- Grutzkau, A. & Radbruch, A. Small but mighty: how the MACS-technology based on nanosized superparamagnetic particles has helped to analyze the immune system within the last 20 years. *Cytometry A* **77**, 643–647, <https://doi.org/10.1002/cyto.a.20918> (2010).
- Momose, F. *et al.* Variant sublines with different metastatic potentials selected in nude mice from human oral squamous cell carcinomas. *J Oral Pathol Med* **18**, 391–395, <https://doi.org/10.1111/j.1600-0714.1989.tb01570.x> (1989).
- Morifuji, M., Taniguchi, S., Sakai, H., Nakabeppu, Y. & Ohishi, M. Differential expression of cytokeratin after orthotopic implantation of newly established human tongue cancer cell lines of defined metastatic ability. *Am J Pathol* **156**, 1317–1326, [https://doi.org/10.1016/S0002-9440\(10\)65002-X](https://doi.org/10.1016/S0002-9440(10)65002-X) (2000).
- Lokaj, J. & John, C. Ilya Ilich Metchnikov and Paul Ehrlich: 1908 Nobel Prize winners for their research on immunity. *Epidemiol Mikrobiol Immunol* **57**, 119–124 (2008).

24. Zembala, M., Ptak, W. & Hanczakowska, M. The role of macrophages in the cytotoxic killing of tumour cells *in vitro*. I. Primary immunization of lymphocytes *in vitro* for target cell killing and the mechanism of lymphocyte-macrophage cooperation. *Immunology* **25**, 631–644 (1973).
25. Komohara, Y., Niino, D., Ohnishi, K., Ohshima, K. & Takeya, M. Role of tumor-associated macrophages in hematological malignancies. *Pathol Int* **65**, 170–176, <https://doi.org/10.1111/pin.12259> (2015).
26. Komohara, Y., Jinushi, M. & Takeya, M. Clinical significance of macrophage heterogeneity in human malignant tumors. *Cancer Sci* **105**, 1–8, <https://doi.org/10.1111/cas.12314> (2014).
27. Kaku, Y. *et al.* Overexpression of CD163, CD204 and CD206 on alveolar macrophages in the lungs of patients with severe chronic obstructive pulmonary disease. *PLoS One* **9**, e87400, <https://doi.org/10.1371/journal.pone.0087400> (2014).
28. Komohara, Y. *et al.* AM-3K, an anti-macrophage antibody, recognizes CD163, a molecule associated with an anti-inflammatory macrophage phenotype. *J Histochem Cytochem* **54**, 763–771, <https://doi.org/10.1369/jhc.5A6871.2006> (2006).
29. Zwadlo-Klarwasser, G., Neubert, R., Stahlmann, R. & Schmutzler, W. Influence of dexamethasone on the RM 3/1-positive macrophages in the peripheral blood and tissues of a New World monkey (the marmoset *Callithrix jacchus*). *Int Arch Allergy Immunol* **97**, 178–180, <https://doi.org/10.1159/000236115> (1992).
30. Fabrick, B. O., Dijkstra, C. D. & van den Berg, T. K. The macrophage scavenger receptor CD163. *Immunobiology* **210**, 153–160, <https://doi.org/10.1016/j.imbio.2005.05.010> (2005).
31. Platt, N. & Gordon, S. Is the class A macrophage scavenger receptor (SR-A) multifunctional? - The mouse's tale. *J Clin Invest* **108**, 649–654, <https://doi.org/10.1172/JCI13903> (2001).
32. Berwin, B. *et al.* Scavenger receptor-A mediates gp96/GRP94 and calreticulin internalization by antigen-presenting cells. *EMBO J* **22**, 6127–6136, <https://doi.org/10.1093/emboj/cdg572> (2003).
33. Azad, A. K., Rajaram, M. V. & Schlesinger, L. S. Exploitation of the Macrophage Mannose Receptor (CD206) in Infectious Disease Diagnostics and Therapeutics. *J Cytol Mol Biol* **1**, <https://doi.org/10.13188/2325-4653.1000003> (2014).
34. Mantovani, A., Bottazzi, B., Colotta, F., Sozzani, S. & Ruco, L. The origin and function of tumor-associated macrophages. *Immunol Today* **13**, 265–270, [https://doi.org/10.1016/0167-5699\(92\)90008-U](https://doi.org/10.1016/0167-5699(92)90008-U) (1992).
35. Goswami, S. *et al.* Macrophages promote the invasion of breast carcinoma cells via a colony-stimulating factor-1/epidermal growth factor paracrine loop. *Cancer Res* **65**, 5278–5283, <https://doi.org/10.1158/0008-5472.CAN-04-1853> (2005).
36. Dong, P. *et al.* CD86(+)/CD206(+), Diametrically Polarized Tumor-Associated Macrophages, Predict Hepatocellular Carcinoma Patient Prognosis. *Int J Mol Sci* **17**, 320, <https://doi.org/10.3390/ijms17030320> (2016).
37. Saito, Y. *et al.* Role of CD204-positive tumor-associated macrophages in adult T-cell leukemia/lymphoma. *J Clin Exp Hematop* **54**, 59–65 (2014).

Acknowledgements

We would like to thank the Research Support Center, Research Center for Human Disease Modeling, Kyushu University Graduate School of Medical Sciences for the technical assistance. And we also appreciate Edanz Group (www.edanzediting.com/ac) for editing a draft of this article. Study conception and design: A.S.M.R.H., M.M., K.K. and S.N. Data acquisition: N.I., A.C., K.M., N.K., T.M. Quality control of data and algorithms: A.S.M.R.H., K.K. and M.S. Data analysis and interpretation: M.M., T.S., S.K. and T.K. Statistical analysis: R.M., T.M., A.T. and J.-N.H. Manuscript preparation and review: M.M. This work was supported by the Japan Society for the Promotion of Science [Grant Numbers 17H04671, 17H01603, 26293430] and “Practical Research Project for Rare/Intractable Diseases,” a matching fund subsidy from the Japan Agency for Medical Research and Development [Grant Number 17ek0109226h0001].

Additional Information

Supplementary information accompanies this paper at <https://doi.org/10.1038/s41598-019-51149-1>.

Competing Interests: The authors declare no competing interests.

Publisher's note Springer Nature remains neutral with regard to jurisdictional claims in published maps and institutional affiliations.



Open Access This article is licensed under a Creative Commons Attribution 4.0 International License, which permits use, sharing, adaptation, distribution and reproduction in any medium or format, as long as you give appropriate credit to the original author(s) and the source, provide a link to the Creative Commons license, and indicate if changes were made. The images or other third party material in this article are included in the article's Creative Commons license, unless indicated otherwise in a credit line to the material. If material is not included in the article's Creative Commons license and your intended use is not permitted by statutory regulation or exceeds the permitted use, you will need to obtain permission directly from the copyright holder. To view a copy of this license, visit <http://creativecommons.org/licenses/by/4.0/>.

© The Author(s) 2019